JOURNAL OF SOLID STATE CHEMISTRY **130,** 311–315 (1997)
ARTICLE NO. SC977391

High-Pressure Synthesis of an Alkali Metal–Transition Metal Laves Phase: KAg_2

M. Hasegawa, T. Atou, J. V. Badding[1]

Department of Chemistry, Pennsylvania State University, University Park, Pennsylvania 16802

Received September 27, 1996; in revised form March 10, 1997; accepted March 12, 1997

A new C14 Laves phase was synthesized by direct reaction of potassium and silver at high pressure in a diamond anvil cell. The structure was refined by Rietveld analysis on powder diffraction data in the space group $P6_3/mmc$ to an R_{F^2} value of 0.034. The lattice parameters are $a = 5.589(5)$ and $c = 9.476(1)$. Formation of this phase under pressure is in agreement with predictions based on Miedema's rules. A novel double-sided laser heating system was developed for the synthesis of KAg_2.

INTRODUCTION

Recently, we have found that the chemistry of the alkali metals can be considerably extended under pressure so that they react with the transition metals (1–3). At ambient pressure, no compounds have been reported to form between the alkali metals potassium, rubidium, and cesium and any of the transition metals other than gold (4, 5). Thus far we have found compounds formed between potassium and nickel (3), palladium (6), and silver (2). We have determined the crystal structures of two potassium silver compounds, K_3Ag, which forms with a cubic BiF_3 type structure, and K_2Ag, which has an anisotropic ω-phase structure (2). Here we report the formation of a third more silver-rich $MgZn_2$ (C14) type Laves phase, KAg_2. Thus, under pressure, the chemical behavior of potassium is substantially altered and the potassium–silver phase diagram becomes much richer, in accordance with predictions based on Miedema's rules (1, 3).

The Laves phases are among the most important classes of intermetallic compounds. A large number of binary intermetallic compounds of stoichiometry AB_2 are known, as well as many ternary phases (4, 5, 7). The Laves phases generally consist of an electropositive metal found near the left side of the periodic table (the A metal) with a more electronegative transition metal (the B metal) (4, 5, 7, 8). The Laves phase reported here is the second reported to form between a heavy alkali metal and a noble metal. The first was KAu_2, which can be synthesized under high pressure (9). Because of their many interesting magnetic and electronic properties and potential uses, such as for hydrogen storage materials (10, 11), a large number of investigations have been performed on Laves phases.

The results presented here demonstrate the versatility of the diamond cell for performing high-pressure syntheses. Key issues in high-pressure synthesis include preparation of homogeneous, well-reacted products, and accurate *in situ* high-pressure structural determination. By use of a novel double-sided laser heating system described below, complete reaction between potassium and silver was effected. Rietveld analyses on diffraction patterns collected using a high-resolution laboratory-based diffraction system allowed thorough characterization of the structure of KAg_2. These techniques should be generally applicable to many high-pressure syntheses. In particular, use of these techniques should allow structural investigations to be performed on a wide variety of compounds formed at high pressures between the alkali metals and transition elements (3). These compounds are of interest because they may exhibit unusual crystal and electronic structures as a result of the transition to directional d electron bonding in the alkali metals under pressure and because of the geophysical implications of their formation.

EXPERIMENTAL

Potassium–silver mixtures of nominal composition KAg_2 were compressed in a Mao–Bell piston–cylinder type diamond anvil cell (12). Loading of the samples was performed in a Vacuum Atmospheres glove box under a high-purity argon atmosphere. Pressure was measured by means of ruby fluorescence (13). Powder diffraction patterns were collected at high pressures with a diffraction system that utilized a Johannson–Guinier quartz monochromator to focus an X-ray beam (Mo$K\alpha_1$, $\lambda = 0.7093$ Å) from a Rikagu RU-200H rotating anode generator onto the sample (14). Because the beam is nearly monochromatic and is

[1] To whom correspondence should be addressed.

0022-4596/97 $25.00

collimated to low divergence, high-quality diffraction data can be collected with this system. The diffraction patterns were collected in the Debeye–Scherrer configuration using DEF-392 X-ray film. The films were scanned into a Macintosh computer and collapsed into diffraction profiles using the program of Meade, Nguyen, and Jeanloz (15).

Compression of the KAg_2 mixture at room temperature to 40 GPa, followed by release of pressure to 7 GPa, resulted in the formation of a phase that, unlike the reactants, exhibited a golden luster. The diffraction pattern from this phase could be indexed with the $MgZn_2$ Laves phase type structure. However, the pattern exhibited broad peaks indicating the presence of disorder, substantial deviatoric stress, phase inhomogeneity, or other structural defects (Fig. 1). In contrast, for the potassium-rich phases in the potassium–silver system, satisfactory reaction could be achieved at room temperature (2). As the fraction of the higher melting silver component is increased, equilibrium becomes more difficult to attain.

In an attempt to improve the quality of the diffraction pattern, the sample was heated using a conventional laser heating system (50 W multimode Nd-YLF laser, 1056 nm). This system heats the sample by focusing the infrared laser beam through the front (cylinder side) diamond. By examination of the color and intensity of the heated spot, the sample temperature was estimated to be in the range of 2000°C. Single-crystal sapphire thermal insulators (~ 8 μm thick) were placed between the diamonds and the sample to avoid thermal damage to the diamonds. If these insulators crack slightly during compression, a small contribution to the diffraction pattern from Al_2O_3 arises. The insulators are chemically inert to pure transition metals and alkali metals (3). Unfortunately, even after laser heating, the quality of the diffraction patterns obtained was still quite poor. When a sample is laser heated through only one diamond, large temperature gradients are present because the rear diamond, which has a high thermal conductivity, serves as an effective heat sink. These temperature gradients inhibit complete reaction and the attainment of equilibrium.

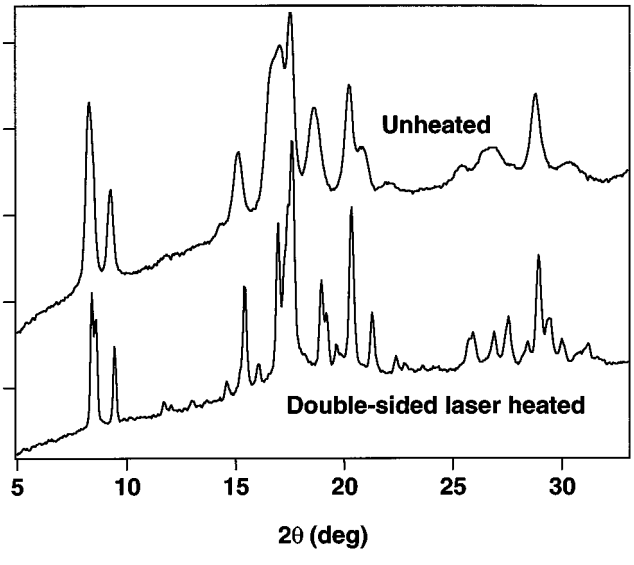

FIG. 1. Diffraction pattern of KAg_2 synthesized by compression at room temperature (top) and by compression and double-sided laser heating (bottom).

To minimize the effect of temperature gradients, the sample was then heated simultaneously through both diamonds at 7 GPa. A double-sided laser heating system was constructed for this purpose. The YLF laser beam was split and focused using two objectives into the front and back of the Mao–Bell cell. Because the numerical aperture available through the back of the diamond cell is small, it was necessary to use a small diameter (6 mm) lens to focus the radiation through this side. Fortunately, even when operated multimode, the beam diameter and divergence of the YLF laser are relatively small, allowing use of a small diameter lens. In contrast, the double-sided laser heating system of Shen and Mao utilizes a large numerical aperature lens and more divergent radiation from a multimode YAG laser (16). This allows a larger, more uniform heating area (advantageous when it is desired to perform *in situ* measurements at high temperature), but requires a diamond cell with a large numerical aperature (e.g., Merrill–Basset type). The diameter of the heated spot in the YLF laser heating system is approximately 40 μm, sufficiently large for synthesis.

Diffraction patterns collected after double-sided laser heating were of much better quality, with sharp, well-resolved peaks (Fig. 1). Some unreacted silver remained in this sample, indicating that the reaction mixture was slightly off stoichiometry. These results for KAg_2 document that double-sided laser heating, a relatively new technique (16), has substantial advantages for synthesis over single sided heating. Without the use of double-sided laser heating, it would not have been possible to perform the structural refinement of KAg_2 presented below.

STRUCTURE DETERMINATION

To confirm the structural assignment and constrain the free positional parameters, a Rietveld refinement of the KAg_2 phase was performed on the diffraction pattern using the program GSAS (17). The intensities of the profiles were corrected for the nonlinear relationship between film density and exposure and for the absorption of the cylinder diamond anvil. Rietveld analyses on standard materials have demonstrated the accuracy of the data collection and correction procedure (2). The diffraction ring profiles on the film were smooth, indicating that a large number of crystallites contributed to the diffraction patterns. The major contribution to the background intensity is Compton

TABLE 1
Crystal Parameters at 20°C

a	5.5891(5)
c	9.4761(1)
c/a	1.6955 (ideal is 1.6333)
V	256.36(5)
Space group	$P6_3/mmc$
Formula weight	254.83 amu
Z	4
d_c	6.603 g/cm^3

scattering from the single-crystal diamond anvils. The step size of the digitized profile was 0.031° (2θ). The refinement included scale, background, lattice, profile, atom position, and isotropic thermal parameters. The peak shapes were modeled using the pseudo-Voight profile function of Thompson *et al.* (18). The silver and sapphire phases were included in the refinement, with refinement of only the phase fraction, thermal parameters, and lattice parameters. The refinement rapidly converged, with agreement factors $R_{wp} = 0.0654$, $R_p = 0.0487$, $\chi^2 = 1.717$, and $R_{F^2} = 0.0340$. Refinement of the atom occupancies resulted in values within 2σ of 1.000, indicating that the stoichiometry KAg_2 is correct. For the final refinements, the occupancies were fixed at 1.000. The crystal and positional parameters at 7 GPa are shown in Tables 1 and 2. A plot of the calculated and observed diffraction profiles is shown in Fig. 2.

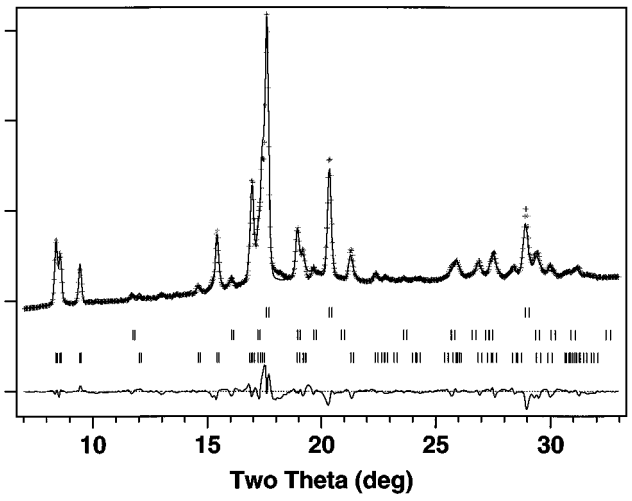

FIG. 2. Diffraction pattern of KAg_2 synthesized by compression and double-sided laser heating (background subtracted). The crosses represent experimental data. The calculated and difference profiles from the Rietveld analysis are drawn as continuous lines. The three sets of tick marks below the pattern represent from top to bottom, the positions of all possible reflections for Ag, Al_2O_3, and KAg_2, respectively.

DISCUSSION

Miedema's rules provide an explanation for the formation of silver–potassium compounds under pressure (1, 3). According to these semi-empirical rules, small differences in electron charge density and large differences in electronegativity (or work function) between two metals favor compound formation (19, 20). The tendency for elements with large differences in electronegativity to form compounds is well documented (19, 20). Large differences in charge density tend to inhibit compound formation because there is a substantial energetic cost in compressing low charge density metals to the density of an intermetallic compound, which is generally intermediate in charge density between its constituent elements.

The electronegativities of the potassium and silver differ considerably. However, the differences in charge density are too large for compound formation at ambient pressure (19, 20). Because it can exhibit a transition to a d^1 electron configuration upon compression (21, 22) and its electron density is low at ambient pressure, potassium is very compressible (23). As a result, under pressure the charge density of potassium increases rapidly, allowing compound formation with silver and many of the other transition metals.

Like other C14 AB_2 Laves phases, KAg_2 contains a sublattice of B atoms (Ag) composed of linked tetrahedra (Fig. 3) that alternately share vertices and faces along the c axis (7). The A atoms (K) form a hexagonal diamond net, composed of boat and chair configuration sixfold rings. One of the chair configuration rings of potassiums surrounding Ag(1) is shown in Fig. 3. An alternative description of the structure is in terms of layers of triangular nets of A and B atoms and Kagome nets, which are composed of triangles and hexagons of B atoms (8). In the ideal C14 Laves phase structure the c/a ratio is 1.63333 and the free positional parameters are $z = 1/6$ and $x = 5/6$ (8). This structure has identical lengths for all of the B–B bonds. The structural parameters for KAg_2 (Table 2) deviate from the ideal values, resulting in small variations in the Ag–Ag interatomic distances in the Ag network (Table 3) and small deviations from the ideal Friaf polyhedra found in Laves phases. The KAu_2 Laves phase also exhibits slight deviations from the ideal structure.

TABLE 2
Positional Parameters

Atom	x	y	z	U_{iso} (Å^2)
K	1/3	2/3	0.07(1)	0.019(8)
Ag(1)	0	0	0	0.031(3)
Ag(2)	0.8286(4)	$2x$	1/4	0.006(1)

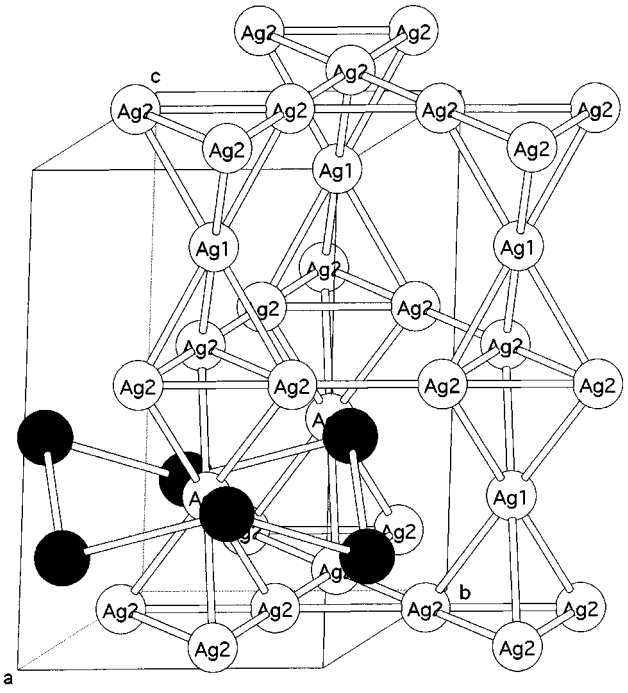

FIG. 3. Crystal structure of KAg_2 drawn using Molview. The *c* axis is tilted slightly from vertical. The black circles represent potassium atoms, most of which have been removed for clarity. The unshaded circles represent silver atoms.

Both geometric and electronic factors have been argued to be important in determining whether the Laves phase structure is adopted and which of the variants ($MgCu_2$, $MgZn_2$, $MgNi_2$) is favored. The ideal radius ratio r_A/r_B for the formation of a binary Laves phase is 1.225, but the observed range of ratios can vary from 1.05 to 1.67 (7). At ambient pressure the radius ratio is 1.576 ($r_K = 2.27$ Å, $r_{Ag} = 1.44$ Å at 0.1 MPa) (7). At 7 GPa, it decreases considerably to 1.340 ($r_K = 1.89$ Å, $r_{Ag} = 1.41$ Å at 7 GPa), indicating that the K atoms are compressed in KAg_2.

Several investigations into the electronic structure of the Laves phases have been performed (8, 24, 25). Johnston and Hoffmann found that for many of the Laves phases there is a complex cyclic relationship between the structure favored (e.g., cubic or hexagonal) and electron count (8). Sharp peaks in the density of states arising from the *B* subnet give rise to this relationship, which was found to be accurate for compounds with *B* atoms from the first row transition metals. Greater discrepancies were noted for compounds composed of second or third row metals, suggesting that a different relationship may be appropriate for these compounds. According to the predictions, KAg_2, with electron count of 23, should adopt the cubic Laves phase structure. However, likely in part because it contains a second row metal, it does not, instead adopting the hexagonal structure.

TABLE 3
Interatomic Distances in KAg_2

	Atom 1	Atom 2	Distance
3	K	K	3.4900(3)
	K	K	3.4085(6)
3	K	Ag(1)	3.2946(3)
6	K	Ag(2)	3.2736(3)
3	K	Ag(2)	3.4150(5)
6	Ag(1)	K	3.2947(3)
6	Ag(1)	Ag(2)	2.8923(4)
4	Ag(2)	K	3.2736(3)
2	Ag(2)	K	3.4150(5)
2	Ag(2)	Ag(1)	2.8923(4)
2	Ag(2)	Ag(2)	2.7154(3)
2	Ag(2)	Ag(2)	2.8738(3)

ACKNOWLEDGMENTS

This work was supported by a National Science Foundation Young Investigator Award, the donors of the Petroleum Research Fund (administered by the American Chemical Society), and a David and Lucile Packard Foundation Fellowship. We thank John Parise for valuable discussions about Rietveld analysis.

REFERENCES

1. J. V. Badding, L. J. Parker, and D. A. Nesting, *J. Solid State Chem.* **117,** 229 (1995).
2. T. Atou, M. Hasegawa, L. J. Parker, and J. V. Badding, *J. Am. Chem. Soc.* **118,** 12104 (1996).
3. L. J. Parker, T. Atou, and J. V. Badding, *Science* **273,** 95 (1996).
4. T. B. Massalski, H. Okamoto, P. R. Subramanian, and L. Kacprzak (Eds.), "Binary Alloy Phase Diagrams," 2nd ed. ASM International, Materials Park, OH, 1990.
5. P. Villars and L. D. Calvert, "Pearson's Handbook of Crystallographic Data for Intermetallic Phases," 2nd ed. ASTM International, Newbury, OH, 1991.
6. L. J. Parker and J. V. Badding, unpublished.
7. A. F. Wells, "Structural Inorganic Chemistry," 5th ed. Clarendon Press, Oxford, 1984.
8. R. L. Johnston and R. L. Hoffmann, *Z. Anorg. Allg. Chem.* **616,** 105 (1992).
9. K. J. Range, F. Rau, and U. Klement, *Acta Crystallogr.* **C 44,** 1485 (1988).
10. V. Z. Mordkovich, Y. K. Baichtok, N. V. Dudakova, E. I. Mazus, and V. P. Mordovin, *J. Alloys Compd.* **231,** 498 (1995).
11. T. Gamo, Y. Tsuji, and Y. Moriwaki, *Proc. Electrochem. Soc.* **94-27,** 155 (1994).
12. A. P. Jephcoat, H. K. Mao, and P. M. Bell, *in* "Hydrothermal Experimental Techniques" (G. C. Ulmer and H. L. Barnes, Eds.), p. 469. Wiley-Interscience, New York, 1987.
13. H. K. Mao, P. M. Bell, J. Shaner, and D. Steinberg, *J. Appl. Phys.* **49,** 3276 (1978).
14. T. Atou and J. V. Badding, *Rev. Sci. Instrum.* **66,** 4496 (1995).
15. J. Nguyen and R. Jeanloz, *Rev. Sci. Instrum.* **64,** 3456 (1993).
16. G. Shen, H. K. Mao, and R. J. Hemley, "Advanced Materials '96—New Trends in High Pressure Research," p. 149. Nat. Inst. Res. Inorganic Mat., Tsukuba, Japan, 1996.

17. A. C. Larson and R. B. Von Dreele, "Report LAUR 86-748, GSAS: General Structure Analysis System," Los Alamos National Laboratory, Los Alamos, NM, 1994.
18. P. Thompson, D. E. Cox, and J. B. Hastings, *J. Appl. Crystallogr.* **20,** 79 (1987).
19. A. R. Miedema, P. F. Chatel, and F. R. de Boer, *Physica B* **100,** 1 (1980).
20. D. G. Pettifor, *Solid State Phys.* **40,** 4392 (1987).
21. H. G. Drickamer, *in* "Solid State Physics" (F. Seitz and D. Turnbull, Eds.), p. 1. Academic Press, New York, 1965.
22. R. M. Sternheimer, *Phys. Rev.* **78,** 235 (1950).
23. D. A. Young, "Phase Diagrams of the Elements," University of California Press, Berkeley, 1991.
24. R. Nesper and G. J. Miller, *J. Alloys Compd.* **197,** 109 (1993).
25. R. Haydock and R. L. Johannes, *J. Phys. F* **5,** 2055 (1975).